

Portland State University

PDXScholar

Physics Faculty Publications and Presentations

Physics

12-2018

High-Performance Self-Powered UV Detector Based on SnO₂-TiO₂ Nanomace Arrays

Duo Chen

School of Physics and State Key Laboratory of Crystal Materials Shandong University Jinan People's Republic of China

Lin Wei

School of Microelectronics Shandong University Jinan People's Republic of China

Lingpan Meng

School of Physics and State Key Laboratory of Crystal Materials Shandong University Jinan People's Republic of China

Yanxue Chen

School of Physics and State Key Laboratory of Crystal Materials Shandong University Jinan People's Republic of China

Yufeng Tian

School of Physics and State Key Laboratory of Crystal Materials Shandong University Jinan People's Republic of China

Follow this and additional works at: https://pdxscholar.library.pdx.edu/phy_fac

 [Click the next page for additional authors](#)
Part of the [Atomic, Molecular and Optical Physics Commons](#)

Let us know how access to this document benefits you.

Citation Details

Chen, D., Wei, L., Meng, L., Wang, D., Chen, Y., Tian, Y., ... & Jiao, J. (2018). High-Performance Self-Powered UV Detector Based on SnO₂-TiO₂ Nanomace Arrays. *Nanoscale research letters*, 13(1), 92.

This Article is brought to you for free and open access. It has been accepted for inclusion in Physics Faculty Publications and Presentations by an authorized administrator of PDXScholar. Please contact us if we can make this document more accessible: pdxscholar@pdx.edu.

Authors

Duo Chen, Lin Wei, Lingpan Meng, Yanxue Chen, Yufeng Tian, Shishen Yan, Liangmo Mei, and Jun Jiao

NANO EXPRESS

Open Access



High-Performance Self-Powered UV Detector Based on SnO₂-TiO₂ Nanomace Arrays

Duo Chen¹, Lin Wei², Lingpan Meng¹, Dong Wang¹, Yanxue Chen^{1*}, Yufeng Tian¹, Shishen Yan¹, Liangmo Mei¹ and Jun Jiao³

Abstract

Abstract: Photoelectrochemical cell-typed self-powered UV detectors have attracted intensive research interest due to their low cost, simple fabrication process, and fast response. In this paper, SnO₂-TiO₂ nanomace arrays composed of SnO₂ nanotube trunk and TiO₂ nanobranches were prepared using soft chemical methods, and an environment-friendly self-powered UV photodetector using this nanostructure as the photoanode was assembled. Due to the synergistic effect of greatly accelerated electron-hole separation, enhanced surface area, and reduced charge recombination provided by SnO₂-TiO₂ nanomace array, the nanostructured detector displays an excellent performance over that based on bare SnO₂ arrays. The impact of the growing time of TiO₂ branches on the performance of UV photodetector was systematically studied. The device based on optimized SnO₂-TiO₂ nanomace arrays exhibits a high responsivity of 0.145 A/W at 365 nm, a fast rising time of 0.037 s, and a decay time of 0.015 s, as well as excellent spectral selectivity. This self-powered photodetector is a promising candidate for high-sensitivity, high-speed UV-detecting application.

Keywords: Self-powered, UV detectors, SnO₂-TiO₂ nanomace arrays, Heterojunction

Background

Ultraviolet photodetectors (UVPDs) have been widely used in many fields, such as remote control, chemical analysis, water purification, flame detection, early missile plume detection, and secure space-to-space communication [1]. To avoid the use of costly UV pass filters and achieve visible-blind operation, wide bandgap semiconductors have been studied widely for light detecting, especially in the ultraviolet region [2]. In recent decades, nanostructured semiconductors such as nanorods, nanowires, nanotubes, and nanobranches have attracted extensive research interest due to their high surface-to-volume ratio and rationally designed surface morphology [3–13]. Photoelectrochemical cell (PEC)-typed photodetectors assembled with nanostructured semiconductors exhibit a high responsivity and a fast transient response compared with traditional photoconductive semiconductor thin film detectors. As a new and efficient way to fabricate high-performance photodetectors,

PEC-based devices can avoid complicated epitaxial processes and expensive single crystal substrates, which is very important for the growing cheaper optoelectronic applications. Therefore, self-powered UVPDs based on PEC device have attracted intensive research interest. Self-powered UVPDs based on PEC structure have been fabricated using a liquid I⁻/I₃⁻ redox couple electrolyte [14–18] and a nanocrystalline TiO₂ film [14] or a multilayer TiO₂ nanorod-assembled cloth/nanorod array-based electrode [15]. Impressive performances were observed in these UVPDs. However, liquid I⁻/I₃⁻ redox couple electrolyte is not ideal for long-term operation: it is highly corrosive, volatile, and photoreactive, interacting with common metallic components and sealing materials. From this point, water-based electrolytes may be the most safe, most stable, and most environment-friendly electrolyte. Zhang et al. have reported a UV-visible photodetector based on ZnO/CuO heterojunctions and NaSO₄ aqueous solution, which shows an excellent photodetection performance [19]. TiO₂ has attracted a great deal of attention due to its outstanding physical and chemical properties for water electrolyte-based UVPDs. Lee et al. reported a UV detector based on a

* Correspondence: cyx@sdu.edu.cn

¹School of Physics and State Key Laboratory of Crystal Materials, Shandong University, Jinan 250100, People's Republic of China

Full list of author information is available at the end of the article

TiO₂ film/water solid–liquid heterojunction [20], which exhibits high photosensitivity, excellent spectral selectivity and fast response. In order to further enlarge the TiO₂/electrolyte contact area, Xie et al. fabricated a self-powered PEC photodetector based on TiO₂ nanorod arrays/water UVPD [21]. Until now, water electrolyte-based UVPDs still show a lower photoresponsivity than those using I[−]/I₃[−] redox couple electrolyte. Moreover, low electron mobility of TiO₂ increases the probability of photon-induced electron recombination with the electrolyte. By contrast, SnO₂ possesses a high electron mobility, suggesting a faster diffusion transport of photon-induced electrons to the transparent conductive oxide current collector. Recently, high-quality TiO₂/SnO₂ heterojunction nanostructures have been prepared by different methods for optoelectronic applications [17, 22]. Impressive performance has been observed in UVPDs using TiO₂/SnO₂ branched heterojunctions and SnO₂ mesoporous spheres @ TiO₂ as electrode materials [16, 17]. However, all these UVPDs were assembled with disordered nanostructures. It can be expected that if ordered SnO₂-TiO₂ nanostructure arrays with a high electron transport efficiency are adopted as the photoanode of the UVPDs, a much better photodetecting performance can be obtained.

In this work, ordered SnO₂-TiO₂ nanomace arrays (STNMAs) was synthesized using soft chemical methods. An environment-friendly self-powered UVPD was assembled using the STNMAs as photoanode and water as electrolyte. The schematic structure of STNMAs/H₂O UVPD is shown in Fig. 1. STNMAs grown vertically on fluorine-doped tin oxide (FTO) glass were used as the active electrode. The STNMA-based device shows a higher photocurrent density than that of the bare SnO₂ nanotube-based device under UV irradiation. The spectral photosensitivity and response time are characterized to evaluate the potential of the STNMA UVPD. The impact of the growing time of TiO₂ branches on the performance of UV photodetector was also studied. The self-powered UVPD based on optimized STNMAs exhibits a high responsivity of 0.145 A/W, a fast rise time of 0.037 s, and a decay time

of 0.015 s, as well as excellent spectral selectivity. Moreover, the electrolyte of this photodetector is water, which is low cost, stable, and environment friendly.

Methods

Synthesis of SnO₂ Nanotube Arrays

FTO glass (2 cm × 2 cm) was ultrasonically cleaned with ethanol and deionized water for 15 min respectively and then dried in the air. A 10-nm Sn film was deposited on FTO by thermal evaporation and annealed in air at 550 °C for 1 h to form a dense SnO₂ layer. High-quality ZnO nanorod arrays were prepared on the SnO₂ buffered FTO glass by a two-step hydrothermal method. The details could be found in our previous work [23]. SnO₂ shell layer was deposited on the ZnO nanorod array by a liquid phase deposition. FTO covered with ZnO nanorod arrays was immersed in Na₂SnO₃ aqueous solution at 60 °C for 1 h. Then the sample was immersed in 0.01 M dilute hydrochloric acid to remove the ZnO template, and uniform SnO₂ nanotube arrays (SNAs) were obtained.

Synthesis of SnO₂-TiO₂ Nanomace Arrays

TiO₂ nanobranches were grown on the SnO₂ nanotube trunk by a simple aqueous chemical growth method. The SnO₂ nanotube arrays on FTO glass prepared above were put in an aqueous solution of 0.2 M TiCl₄ at room temperature. In order to achieve different TiO₂ nanobranch length, the deposition was conducted at 6, 12, 18, and 24 h respectively. The resulted STNMAs were thoroughly rinsed with deionized water and then annealed at 450 °C for 30 min.

Assemble of the UV Detector

The PEC-typed photodetector was assembled in a similar structure of a dye-sensitized solar cell, as discussed in our previous work [24]. In brief, the obtained STNMAs synthesized on FTO glass were used as the active electrode and a 20-nm-thick Pt film deposited on FTO glass by magnetron sputtering is adopted as the counter electrode. The active electrode (SnO₂/FTO) and the counter electrode (Pt/FTO) were adhered together face to face with a 60-μm-thick sealing material (SX-1170-60, Solaronix SA, Aubonne, Switzerland). Finally, deionized water was injected into the space between the top and counter electrodes. The effective area of the UV detector was approximately 0.2 cm².

Characterization

The crystal structure of the samples was examined by X-ray diffraction (XRD; XD-3, PG Instruments Ltd., Beijing, China) with Cu Kα radiation (λ = 0.154 nm). The surface morphology of the samples was characterized using a field emission scanning electron microscope

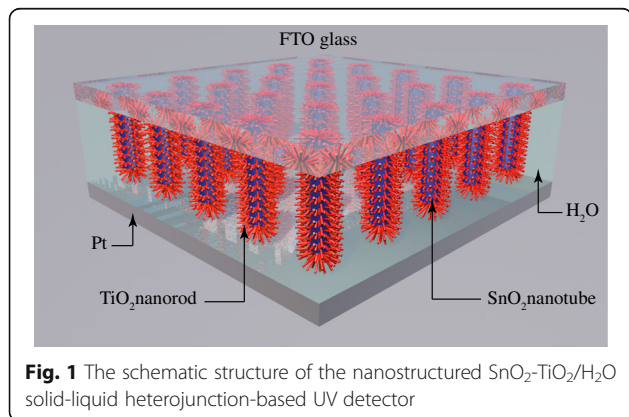


Fig. 1 The schematic structure of the nanostructured SnO₂-TiO₂/H₂O solid-liquid heterojunction-based UV detector

(FESEM; Hitachi S-4800, Hitachi, Ltd., Chiyoda, Tokyo, Japan) and a transmission electron microscope (TEM; F-20, FEI Company, Hillsboro, OR, USA). The optical transmittance was measured using an UV-visible dual beam spectrophotometer (TU-1900, PG Instruments, Ltd., Beijing, China). A 500-W Xenon lamp (7ILX500, 7Star Optical Instruments Co., Beijing, China) with a monochromator (7ISW30, 7Star Optical Instruments Co.) was used as UV light source to generate monochromatic light for the spectral response characterization. The spectral photoresponse characteristics were obtained by a programmable sourcemeter (2400, Keithley Instruments Inc., Cleveland, OH, USA). The photoresponse switching behavior measurement was obtained by an electrochemical workstation (RST5200, Zhengzhou Shirusi Instrument Technology Co. Ltd., Zhengzhou, China).

Results and Discussion

Morphology of SnO₂ nanotube arrays (SNAs) and STNMAs was examined by a FESEM. As shown in Fig. 2a, ordered SNAs with opened top were grown uniformly on the surface of FTO glass substrate. Further analysis

indicates that the nanotubes have a diameter of 50–80 nm and a wall thickness less than 10 nm. The density of nanotubes is typically 30 nanotube/ μm^2 . Figure 2b–e illustrates the SnO₂ nanotube arrays immersed in TiCl₄ solution for 6, 12, 18, and 24 h, respectively. It can be clearly seen that the SnO₂ nanotubes grow almost vertically to the FTO substrate and are covered with a large number of TiO₂ nanobranched to form a nanomace structure. The morphology of SNA and STNMA is also checked by TEM. As shown in Fig. 2g, h for the bare SNA and STNMA grown for 18 h, the SnO₂ nanotube has a length of about 500 nm and the TiO₂ branches grow tightly on the wall of SnO₂ nanotubes. The morphology of the STNMAs is strongly dependent on the growth time. As the growth time increased, the branches become more numerous and longer. These nanobranched coated on SnO₂ nanotube would greatly enlarge the specific surface area and roughness, which is important for PEC applications. However, once the deposition time reaches 24 h or longer, the branches will form continuous network that greatly suppresses the effective active area, which would result in a decrease of the active area of TiO₂ contacted with the electrolyte. This is confirmed by the reduced performance

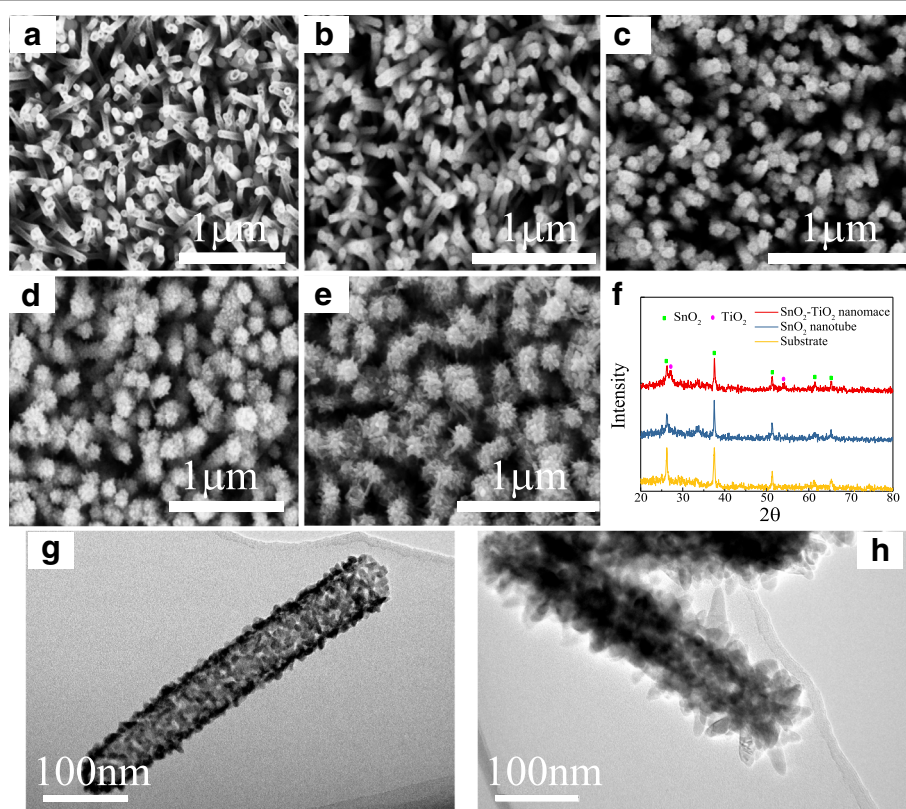


Fig. 2 SEM and TEM images and XRD patterns of SnO₂ nanotube arrays and SnO₂-TiO₂ nanomace arrays. **a** High-magnification top-view SEM image of SnO₂ nanotube arrays. **b** SEM image of 6-h-grown STNMAs. **c** SEM image of 12-h-grown STNMAs. **d** SEM image of 18-h-grown STNMAs. **e** SEM image of 24-h-grown STNMAs. **f** X-ray diffraction patterns of the substrate, SnO₂ nanotube arrays, and STNMAs. **g** TEM image of bare SNA. **h** TEM image of 18-h-grown STNMAs

of the photodetector in the following part. The crystal structure of the SNAs and STNMAs with 18 h deposition time was examined by X-ray diffraction (XRD), and the corresponding patterns are presented in Fig. 2f. The 2θ scan pattern shows that all the peaks of the SnO_2 nanotubes is consistent with those of the FTO substrate, which can be indexed to SnO_2 rutile structure [JCPDS No. 77-0450.]. After the deposition of TiO_2 nanobranched, two more peaks appear, corresponding to the (110) and (211) planes of the rutile TiO_2 [JCPDS No. 02-0494.]. The XRD results indicate that the STNMAs are composed of rutile SnO_2 nanotube trunk and rutile TiO_2 nanobranched without other phases.

The transmission spectrum of the FTO glass, SNAs, and STNMAs is shown in Fig. 3a. A sharp absorption edge located at 320 nm can be observed for FTO glass. The absorption edge of SnO_2 nanotube arrays and 6-h-grown STNMAs is similar to that of the FTO glass, but the absorption edge of 12–24-h-grown STNMAs all show an obvious red shift. The transmittance of FTO reaches to zero when the wavelength is shorter than 305 nm, which determines the spectral response edge in the short-wavelength region. The strong light scattering by the TiO_2 nanobranched causes a lower transmittance of all STNMAs than that of FTO and SnO_2 nanotubes in the wavelength range of 400–550 nm. From these transmittance spectra, it can be concluded that only light with the wavelength between 305 and 400 nm can be well absorbed by TiO_2 arrays and contribute to the UV photoresponsivity, which is confirmed in the following spectral response characterization. The spectral responsivity of these photodetectors was measured in the range of 300–550 nm at zero bias, as shown in Fig. 3b. The responsivity is calculated by the following formula: $R = I/AE$, where R is the responsivity, I is the measured photocurrent, A is the active area of the photodetector device, and E is the irradiance intensity of the light source,

which is measured by a standard light power meter. The device performs as a self-powered photodetector that operates at a nominal zero-applied voltage, with a large photocurrent response under a weak light illumination. As shown in Fig. 3b, the maximum responsivity value for a bare SNA-based UV photodetector is approximately 0.01 A/W at 335 nm, corresponding to an incident photon-to-current conversion efficiency (IPCE) of only 3.7%. Normally, oxygen vacancy can be easily formed in SnO_2 material and cause a high charge recombination. TiO_2 nanobranched deposition on the SNAs can passivate the surface of SnO_2 and reduce the electron-hole recombination. The STNMA-based photodetectors show much better UV photoresponsivity. The peak responsivity of STNMAs grown for 18 h is approximately 0.145 A/W at 365 nm. The corresponding IPCE is higher than 49.2%, which is much higher than other H_2O -based PEC detectors at this wavelength [20, 23, 24]. Considering the loss of incident photons caused by the light absorption and scattering of the FTO glass, much higher internal quantum efficiency can be expected. The TiO_2 nanobranched coated on the SnO_2 nanotube arrays greatly increase not only the contact interface area between the STNMAs and the electrolyte but also the light scattering ability, resulting in an enhancement of the photon harvesting efficiency. Furthermore, these ultrathin branches are very effective at transporting holes to the TiO_2 /water interface as most electron-hole pairs are formed within the diffusion length, ultimately minimizing the recombination loss. Moreover, the photoelectrons injected into SnO_2 nanotube from TiO_2 nanobranched reach the FTO collecting electrode rapidly because SnO_2 possesses a higher electron mobility than TiO_2 . When the growth time reaches 24 h or longer, the branches on the nanotube arrays are interconnected. The active area of TiO_2 contacted with the electrolyte decreases. Therefore, an excessively long

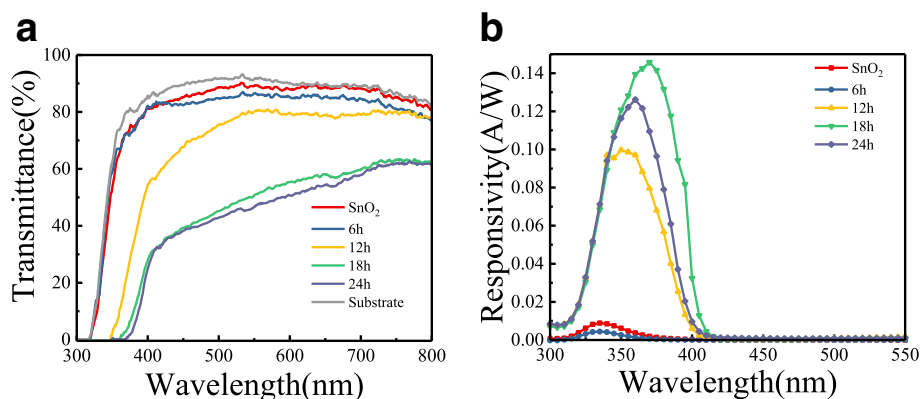


Fig. 3 The UV-visible transmittance spectra and responsivity spectrum of photodetectors. **a** Spectrum of transmittance for FTO glass substrate, SNAs, and STNMAs with different growth time. **b** Responsivity spectrum of photodetectors based on SNAs and STNMAs

growth time is disadvantageous and leads to a reduced photovoltaic performance of the UV photodetector.

To characterize their responsivity to a fast-changing light signal, the photocurrent density-time characteristics of the devices were measured at 0 V bias under an intermittent 365 nm UV-light irradiation with a power of $129 \mu\text{W}/\text{cm}^2$. The incident radiation is switched with an on/off interval of 10 s. Five repeated cycles are displayed in Fig. 4a, which indicates that the photocurrent can be reproducibly switched between the “ON” state and the “OFF” state by periodically turning the UV light on and off. When the deposition time of TiO_2 nanobranched is less than 6 h, the photocurrent density is quite low. In this case, only TiO_2 nanoparticles with a high defect density were formed on the surface of SnO_2 nanotube, which would result in a high electron-hole recombination and a poor photoresponse. With the increase of growth time, the crystal quality of the TiO_2 nanobranched was improved and the surface area was greatly increased. Therefore, the photocurrent has a significant increase when the growth time is longer than 6 h and reaches the maximum when the deposition time is 18 h. From the enlarged rising and

decaying time of the UV detector are approximately 0.037 and 0.015 s (Fig. 4b, c), indicating a rapid photoresponse characteristic. The quantitative criterion for the rising time is the time to reach 90% of the stable photocurrent, and that for decay time is time to reach $1/e$ (37%) of the original photocurrent. The overall performance of the STNMA-based self-powered UV detector is considerably better than that reported by other works, as compared in Table 1.

Schematic diagram of energy band matching and device working mechanism are shown in Fig. 5. When the incident light travels through FTO glass and reaches the active layer of TiO_2 nanobranched, photons with energy exceeding the TiO_2 bandgap will be absorbed and electrons are excited from the valance band to the conduction band, and electron-hole pairs will be generated thereafter. The built-in potential across the interface works as the driving force to separate the electron-hole pairs. Negative electrons move along from TiO_2 nanobranched to the SnO_2 nanotube and get collected by the FTO electrode. These electrons will easily transfer into the external circuit and return to the Pt layer of the counter electrode since the work function of FTO matches with the conduction band of SnO_2 and TiO_2 .

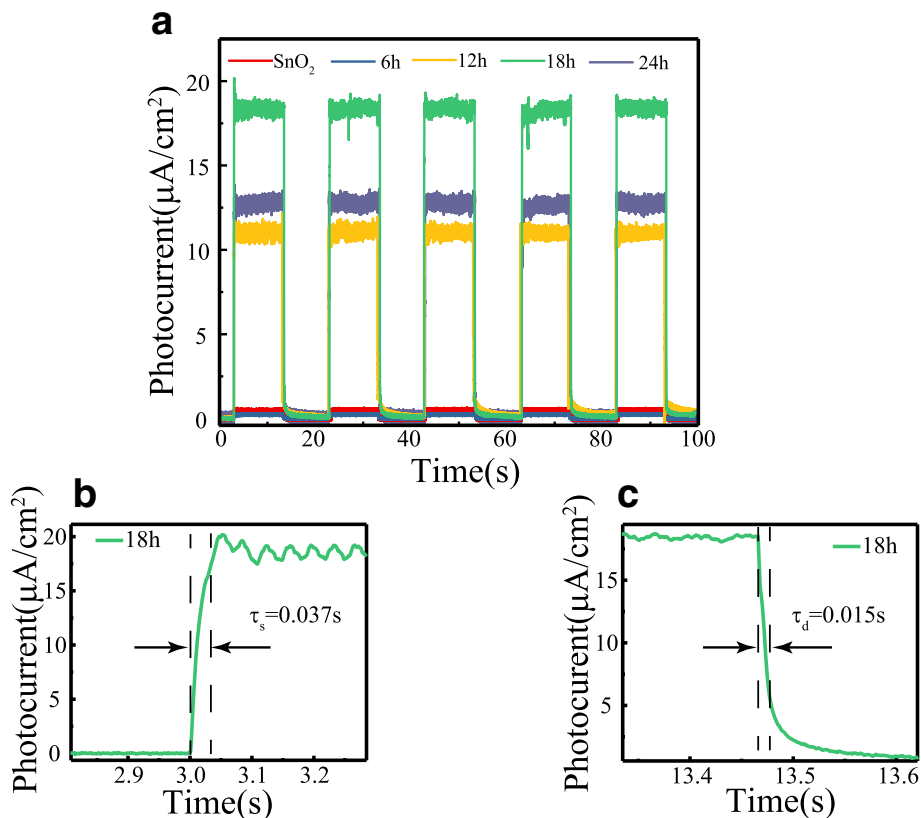


Fig. 4 Time response of the STNMAs/water UV detector. **a** Photocurrent response under on/off radiation of $129 \mu\text{W}/\text{cm}^2$ UV light illumination. **b** Enlarged rising and **c** decaying edge of the photocurrent response

Table 1 Comparison of the self-powered UVPDs with other works

Electrode	Electrolyte	Wavelength of peak (nm)	Responsivity (A/W)	Efficiency (%)	Rising time (s)	Decay time (s)	Reference
SnO ₂ mesoporous spheres@TiO ₂	I ⁻ /I ₃ ⁻	350	0.113	42.6	0.007	0.006	[16]
SnO ₂ nanotube-TiO ₂	I ⁻ /I ₃ ⁻	350	–	20	–	–	[25]
TiO ₂ nanorod arrays	H ₂ O	365	0.025	8.4	0.15	0.05	[20]
ZnO nanoneedle arrays	H ₂ O	385	0.022	7.1	0.1	0.1	[24]
ZnO nanorod-ZnS arrays	H ₂ O	340	0.056	20.4	0.02	0.04	[23]
SnO ₂ -TiO ₂ nanomace arrays	H ₂ O	365	0.145	49.2	0.037	0.015	This work

The positive holes are driven to the surface of the TiO₂ nanobranched and get captured by OH⁻ anion, the reduced form of the redox molecule ($h^+ + OH^- \rightarrow OH\cdot$). Fast removal of holes can be expected across the heterojunction due to the large surface area. The oxidized form of the redox molecule is reduced back to the reduced form OH⁻ at the counter electrode (Pt/FTO) by the electrons that re-entered into the UV detector from the external circuit ($e^- + OH\cdot \rightarrow OH^-$). Here the Pt serves as both a catalyst for the redox reaction and conducting road for the electrons. The circuit was completed in this manner, demonstrating a self-powered UV detection property.

Conclusions

In summary, we have synthesized SnO₂-TiO₂ nanomace arrays composed of SnO₂ nanotube trunk and TiO₂ nanobranched using soft chemical methods. A self-powered UV detector was assembled using this nanostructure as the active electrode and water as the electrolyte. Due to the accelerated electron-hole separation speed by the SnO₂-TiO₂ core-shell structure, enlarged surface area of TiO₂ nanobranched, and fast electron transport property of SnO₂ nanotube, an excellent performance was obtained in this nanostructured

photodetector. For the detector based on the optical STNMAs, a high IPCE up to 49.2% is observed at 365 nm, which is more than 10 times larger than the maximum IPCE of bare SnO₂ nanotube (3.7%). A rapid response time and an excellent spectral selectivity were also obtained in this photodetector. We believe that this SnO₂-TiO₂ nanomace structure can be extended to other applications based on photoelectrochemical effect, such as dye-sensitized solar cells and photoelectrochemical hydrogen production.

Abbreviations

FTO: Fluorine-doped tin oxide; IPCE: Incident photon-to-current conversion efficiency; PEC: Photoelectrochemical cell; SEM: Scanning electron microscope; SNAs: SnO₂ nanotube arrays; STNMAs: SnO₂-TiO₂ nanomace arrays; TEM: Transmission electron microscope; UV: Ultraviolet; UVPDs: Ultraviolet photodetectors; XRD: X-ray diffraction

Acknowledgements

This work was supported by the National Key R&D Program of China (2016YFA0301204), the National Natural Science Foundation of China (11774202, 51231007), and the 111 Project (B13029).

Funding

Funding was received from the National Key R&D Program of China (2016YFA0301204), National Natural Science Foundation of China (11774202, 51231007), and the 111 Project (B13029).

Availability of Data and Materials

The authors declare that materials and data are promptly available to readers without undue qualifications in material transfer agreements. All data generated or analyzed during this study are included in this article.

Authors' Contributions

The work presented here was performed in collaboration of all authors. DC carried out the measurements of the STNMAs/water UV detector and drafted the manuscript. LW conducted the transmittance spectra measurements. LPM grew the SNAs. DW carried out the XRD and the SEM characterizations. YC supervised the work and finalized the manuscript. SY and YT analyzed the results and participated in the revision of the manuscript. LMM and JJ proofread the manuscript and corrected the English. All authors read and approved the final manuscript.

Authors' Information

DC and DW are doctoral students of Shandong University. LPM is a master student of Shandong University. LW is a lecturer of Shandong University. YC, YT, SY, and LMM are professors of Shandong University. JJ is a professor of Portland State University.

Competing Interests

The authors declare that they have no competing interests.

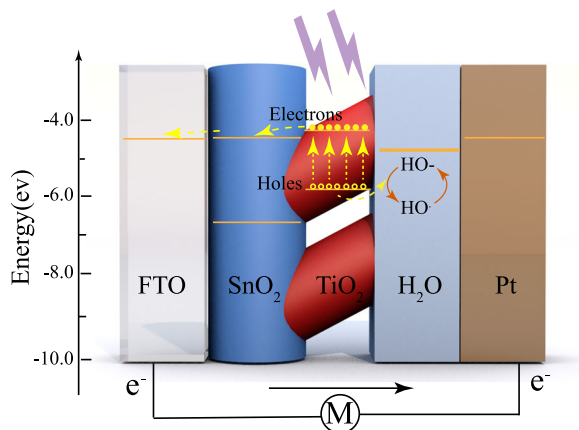


Fig. 5 Schematic energy band diagram and the electron-transfer processes for the STNMAs/H₂O heterojunction

Publisher's Note

Springer Nature remains neutral with regard to jurisdictional claims in published maps and institutional affiliations.

Author details

¹School of Physics and State Key Laboratory of Crystal Materials, Shandong University, Jinan 250100, People's Republic of China. ²School of Microelectronics, Shandong University, Jinan 250100, People's Republic of China. ³Department of Mechanical and Materials Engineering, Portland State University, P.O. Box 751, Portland, OR 97207-0751, USA.

Received: 18 January 2018 Accepted: 27 March 2018

Published online: 03 April 2018

References

- Munoz E, Monroy E, Pau JL, Calle F, Omnes F, Gibart P (2001) III nitrides and UV detection. *J Phys-Condens Mat* 13:7115–7137
- Monroy E, Omnes F, Calle F (2003) Wide-bandgap semiconductor ultraviolet photodetectors. *Semicond Sci Technol* 18:R33–R51
- Game O, Singh U, Kumari T, Banpurkar A, Ogale S (2014) ZnO(N)-Spiro-MeOTAD hybrid photodiode: an efficient self-powered fast-response UV (visible) photosensor. *Nano* 6:503–513
- Lin P, Yan X, Zhang Z, Shen Y, Zhao Y, Bai Z, Zhang Y (2013) Self-powered UV photosensor based on PEDOT:PSS/ZnO micro/nanowire with strain-modulated photoresponse. *ACS Appl Mater Interfaces* 5:3671–3676
- Yang Y, Guo W, Qi J, Zhao J, Zhang Y (2010) Self-powered ultraviolet photodetector based on a single Sb-doped ZnO nanobelt. *Appl Phys Lett* 97:223113
- Cao C, Hu C, Wang X, Wang S, Tian Y, Zhang H (2011) UV sensor based on TiO₂ nanorod arrays on FTO thin film. *Sensor Actua B-Chem* 156:114–119
- Bie YQ, Liao ZM, Zhang HZ, Li GR, Ye Y, Zhou YB, Xu J, Qin ZX, Dai L, Yu DP (2011) Self-powered, ultrafast, visible-blind UV detection and optical logical operation based on ZnO/GaN nanoscale p-n junctions. *Adv Mater* 23:649–653
- Lu S, Qi J, Liu S, Zhang Z, Wang Z, Lin P, Liao Q, Liang Q, Zhang Y (2014) Piezotronic interface engineering on ZnO/au-based Schottky junction for enhanced photoresponse of a flexible self-powered UV detector. *ACS Appl Mater Interfaces* 6:14116–14122
- Hassan JJ, Mahdi MA, Kasim SJ, Ahmed NM, Abu Hassan H, Hassan Z (2012) High sensitivity and fast response and recovery times in a ZnO nanorod array/p-Si self-powered ultraviolet detector. *Appl Phys Lett* 101:261108
- Xia Y, Yang P, Sun Y, Wu Y, Mayers B, Gates B, Yin Y, Kim F, Yan H (2003) One-dimensional nanostructures: synthesis, characterization, and application. *Adv Mater* 15:353–389
- Jie JS, Zhang WJ, Jiang Y, Meng XM, Li YQ, Lee ST (2006) Photoconductive characteristics of single-crystal CdS nanoribbons. *Nano Lett* 6:1887–1892
- Soci C, Zhang A, Xiang B, Dayeh SA, Aplin DPR, Park J, Bao XY, Lo YH, Wang D (2007) ZnO nanowire UV photodetectors with high internal gain. *Nano Lett* 7:1003–1009
- Luo J, Ma L, He T, Ng CF, Wang S, Sun H, Fan HJ (2012) TiO₂/(CdS, CdSe, CdSeS) nanorod heterostructures and photoelectrochemical properties. *J Phys Chem C* 116:11956–11963
- Li X, Gao C, Duan H, Lu B, Pan X, Xie E (2012) Nanocrystalline TiO₂ film based photoelectrochemical cell as self-powered UV-photodetector. *Nano Energy* 1:640–645
- Wang Z, Ran S, Liu B, Chen D, Shen G (2012) Multilayer TiO₂ nanorod cloth/nanorod array electrode for dye-sensitized solar cells and self-powered UV detectors. *Nano* 4:3350–3358
- Huang Y, Yu Q, Wang J, Li X, Yan Y, Gao S, Shi F, Wang D, Yu C (2015) A high-performance self-powered UV photodetector based on SnO₂ mesoporous spheres @ TiO₂. *Electronic Mater Lett* 11:1059–1065
- Li X, Gao C, Duan H, Lu B, Wang Y, Chen L, Zhang Z, Pan X, Xie E (2013) High-performance photoelectrochemical-type self-powered UV photodetector using epitaxial TiO₂/SnO₂ branched heterojunction nanostructure. *Small* 9:2005–2011
- Gao C, Li X, Wang Y, Chen L, Pan X, Zhang Z, Xie E (2013) Titanium dioxide coated zinc oxide nanostrawberry aggregates for dye-sensitized solar cell and self-powered UV-photodetector. *J Power Sources* 239:458–465
- Bai Z, Zhang Y (2016) Self-powered UV-visible photodetectors based on ZnO/Cu₂O nanowire/electrolyte heterojunctions. *J Alloys Compd* 675:325–330
- Xie Y, Wei L, Wei G, Li Q, Wang D, Chen Y, Yan S, Liu G, Mei L, Jiao J (2013) A self-powered UV photodetector based on TiO₂ nanorod arrays. *Nanoscale Res Lett* 8:188
- Lee WJ, Hon MH (2011) An ultraviolet photo-detector based on TiO₂/water solid-liquid heterojunction. *Appl Phys Lett* 99:251102
- Miller DR, Akbar SA, Morris PA (2017) Synthesis of hierarchical SnO₂ nanowire-TiO₂ nanorod brushes anchored to commercially available FTO-coated glass substrates. *Nano-Micro Lett* 9:33
- Lin H, Wei L, Wu C, Chen Y, Yan S, Mei L, Jiao J (2016) High-performance self-powered photodetectors based on ZnO/ZnS core-shell nanorod arrays. *Nanoscale Res Lett* 11:420
- Li Q, Wei L, Xie Y, Zhang K, Liu L, Zhu D, Jiao J, Chen Y, Yan S, Liu G, Mei L (2013) ZnO nanoneedle/H₂O solid-liquid heterojunction based self-powered ultraviolet detector. *Nanoscale Res Lett* 8:415
- Hou X, Wang X, Liu B, Wang Q, Wang Z, Chen D, Shen G (2014) SnO₂@TiO₂ heterojunction nanostructures for lithium-ion batteries and self-powered UV photodetectors with improved performances. *ChemElectroChem* 1:108–115

Submit your manuscript to a SpringerOpen® journal and benefit from:

- Convenient online submission
- Rigorous peer review
- Open access: articles freely available online
- High visibility within the field
- Retaining the copyright to your article

Submit your next manuscript at ► springeropen.com